ORGANOMETALLICS

pubs.acs.org/Organometallics

Article

Nickel Hydride Complexes Supported by a Pyrrole-Derived Phosphine Ligand

Joel D. Collett, Jeanette A. Krause, and Hairong Guan*

Cite This: *Organometallics* 2022, 41, 345−353

Read Online

ACCESS | Metrics & More | Article Recommendations | Supporting Information

ABSTRACT: The synthesis of two nickel hydride complexes bearing the pyrrole-derived phosphine ligand $^{Cy}PN^H$ (2-(dicyclohexylphosphino)methyl-1*H*-pyrrole) was developed, namely, $(\kappa^P\text{-}^{Cy}PN^H)(\kappa^P,\kappa^N\text{-}^{Cy}PN)NiH$ and the acid-stable *trans*-$(\kappa^P\text{-}^{Cy}PN^H)_2Ni(OAc)H\cdot HOAc$. $(\kappa^P\text{-}^{Cy}PN^H)(\kappa^P,\kappa^N\text{-}^{Cy}PN)NiH$ stoichiometrically reduces benzaldehyde and acetophenone in a metal−ligand cooperative manner and catalytically dimerizes ethylene and cycloisomerizes 1,5-cyclooctadiene and 1,5-hexadiene. *trans*-$(\kappa^P\text{-}^{Cy}PN^H)_2Ni(OAc)H\cdot HOAc$, available from the protonation of $(\kappa^P\text{-}^{Cy}PN^H)(\kappa^P,\kappa^N\text{-}^{Cy}PN)NiH$ with acetic acid, catalyzes the cycloisomerization of 1,5-cyclooctadiene more effectively and produces the less thermodynamically favored cycloisomers of 1,5-cyclooctadiene.

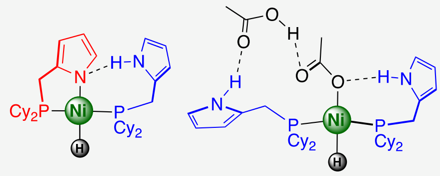

■ INTRODUCTION

Nickel hydride species play important roles in nickel-catalyzed reactions that employ H_2, boranes, or silanes. Well-defined nickel hydride complexes often rely on the use of multidentate ligands with sufficient steric bulk to protect the Ni−H moiety.[1] Our early work focusing on the bis(phosphinite)-based ligand platform[2] allowed us to access pincer-type nickel hydride complexes (Figure 1), provided that the phosphorus substituents are sterically demanding (R = *tert*-butyl, isopropyl, or cyclopentyl groups). An attempted synthesis of $\{\kappa^P,\kappa^C,\kappa^P\text{-}2,6\text{-}(Ph_2PO)_2C_6H_3\}NiH$ with a more exposed Ni−H bond led to intractable products.[3] The pyrrole-based PNP-pincer system studied by Gade,[4] Tonzetich,[5] Bernskoetter,[6] and Walter[6] shows very similar behavior. While nickel hydrides can be stabilized by a bulky pyrrolyl-linked diphosphine, changing the phosphorus substituents from *tert*-butyl or cyclohexyl to phenyl groups yields a hydride species that degrades rapidly under ambient conditions (Figure 1).[4]

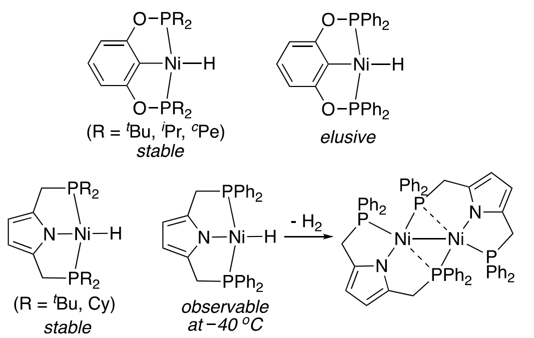

Figure 1. Selected nickel hydride complexes bearing a pincer ligand.

The square-planar geometry, coupled with the rigid ligand framework, limits the reactivity of these pincer-ligated nickel hydrides to insertion reactions involving significantly polarized double bonds, such as those in aldehydes,[3,7] ketones,[3] CO_2,[5,6,8] and CS_2.[9] To regenerate the nickel hydrides, as required for a catalytic reduction process, an oxophilic hydride donor (e.g., a silane or a borane) is often needed to cleave the Ni−O or Ni−S bonds formed during the insertion step.[10] Because of the lack of a vacant coordination site, activation of H_2 by a square-planar nickel alkoxide intermediate proves to be difficult.[11]

The objective of this research is to "dissect" one of the pincer arms so that phosphine (or phosphinite) dissociation becomes realistic, which makes the nickel center more accessible not only for the insertion step but during the hydride regeneration step. The target nickel hydride complexes supported by an LX-type ligand along with a phosphine have precedents in the literature (Figure 2),[12] although none contain an aryl or a pyrrolyl donor that resemble the pincer systems described earlier. To date, we have yet to succeed in preparing the desired phosphinite derivatives, despite the fact that nickel *bromide* complexes bearing a cyclometalated phosphinite along with an L-type ligand can be made.[13] However, we have successfully synthesized a nickel hydride complex, as illustrated in Figure 2, and its derivative from a pyrrole-based phosphine. This compound features a κ^2-P,N-ligand that may undergo ligand dearomatization[14] and a monocoordinating phosphine with a dangling pyrrole group that may participate in secondary coordination sphere

Received: December 14, 2021
Published: February 3, 2022

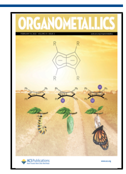

https://doi.org/10.1021/acs.organomet.1c00694
Organometallics 2022, 41, 345−353

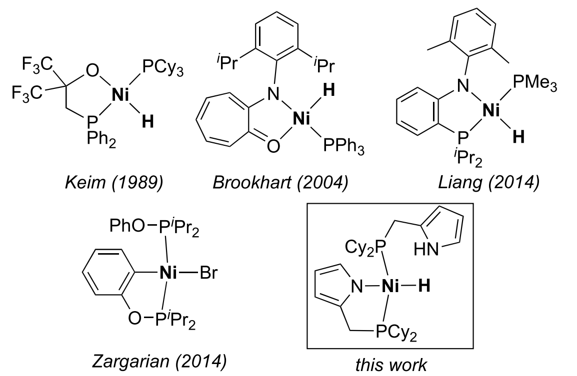

Figure 2. Nickel hydride complexes supported by an LX-type ligand along with a phosphine as well as the related nickel *bromide* complex.

interactions.[15] Its synthesis, characterization, and catalytic applications are the subject of this report.

■ RESULTS AND DISCUSSION

The PNP-pincer system taught us that the *P*-cyclohexyl-substituted ligand could strike a balance between stabilizing the nickel hydride and allowing it to react.[5,6] We thus focused on the use of 2-(dicyclohexylphosphino)methyl-1*H*-pyrrole ($^{Cy}PN^{H}$ for short) to build nickel hydride complexes. This specific ligand was previously reported by Bochmann in a four-step synthesis from pyrrole-2-carboxaldehyde following *N*-BOC (BOC = *tert*-butyloxycarbonyl) protection, C−P bond formation with Cy_2PH to yield a phosphine oxide, *N*-BOC deprotection, and $LiAlH_4$ reduction to unmask the phosphine.[16] We developed a more expedited synthesis through a $Me_2N \rightarrow Cy_2P$ substitution reaction between 2-(dimethylamino)methyl-1*H*-pyrrole (available from the Mannich reaction of pyrrole with HCHO and $Me_2NH{\cdot}HCl$[17]) and Cy_2PH (Scheme 1). This strategy is analogous to the one adopted by several research groups to prepare the pyrrole-based PNP-pincer ligands.[5,6,18]

Scheme 1. Synthetic Route to the Hydride Complex 1

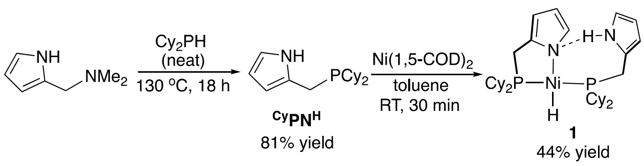

With the target ligand in hand, we treated Ni(1,5-COD)$_2$ (1,5-COD = 1,5-cyclooctadiene) with 2 equiv of $^{Cy}PN^{H}$ (Scheme 1), which resulted in the isolation of a nickel hydride complex formulated as (κ^P-$^{Cy}PN^H$)(κ^P,κ^N-^{Cy}PN)NiH (**1**, ^{Cy}PN denotes the NH-deprotonated ligand). We note that no other nickel hydride species could be detected during this process, even when only 1 equiv of $^{Cy}PN^{H}$ was employed. The presence of a hydride ligand in **1** was confirmed by a Ni−H vibrational band observed at 1912 cm^{-1} and a proton NMR resonance located at −20.78 ppm (in C_6D_6). The molecule contains two inequivalent phosphorus centers, as suggested by the splitting pattern of the hydride resonance (a doublet of doublets) and an AB spin system displayed in the $^{31}P\{^1H\}$ NMR spectrum. The evidence to support the presence of a pendant pyrrole group came from an NH proton resonance found at 9.31 ppm, which is downfield shifted by 1.67 ppm from that of the free ligand (in C_6D_6), possibly due to a slightly enhanced hydrogen bond formation. No dynamic behavior was observed in the temperature range of 25−90 °C (using toluene-d_8 as the solvent).

The molecular structure of **1** was more firmly established by X-ray crystallography. As illustrated in Figure 3, nickel is situated in a distorted square-planar coordination sphere. The distortion is at least in part caused by a *weak* hydrogen-bonding interaction between the pyrrolyl nitrogen (i.e., N1) and the NH functionality of the pendant pyrrole group (2.59(2) Å for the N1···H distance).[19] It appears that, to accommodate the N1···H−N2 interaction, the N1 atom is displaced out of the P1−Ni−P2-H plane, away from the NH functionality, by 0.21(3) Å, and the pyrrolyl ring (N1−C2−C3−C4−C5) is also orientated away to have a dihedral angle of 24.81(5)° with the P1−Ni−P2−H plane.

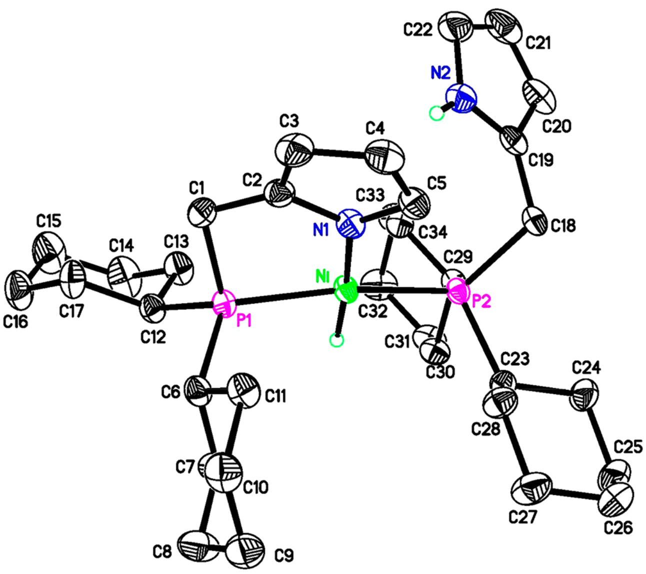

Figure 3. ORTEP drawing of (κ^P-$^{Cy}PN^H$)(κ^P,κ^N-^{Cy}PN)NiH (**1**) at the 50% probability level (all hydrogen atoms except those bound to nitrogen and nickel are omitted for clarity). Selected interatomic distances (Å) and angles (deg): Ni−N(1) 1.9105(9), Ni−P(1) 2.1491(3), Ni−P(2) 2.1653(3), Ni−H 1.390(18), N(2)−H 0.81(2), N(1)···N(2) 3.322(1), N(1)···H 2.59(2); P(1)−Ni−P(2) 167.340(14), N(1)−Ni−P(1) 85.39(3), N(1)−Ni−P(2) 107.27(3), P(1)−Ni−H 88.7(7), P(2)−Ni−H 78.7(7), N(1)···H−N(2) 151(2).

The presence of both a hydridic hydrogen and a relatively acidic pyrrole hydrogen within the same molecule invokes the possibility of metal−ligand cooperative (MLC) reactivity.[20] While complex **1** does not appear to react with CO_2 (1 bar, 80 °C, 20 h), it reduces benzaldehyde and acetophenone in an MLC fashion by transferring both H$^-$ and H$^+$ to the carbonyl group (Scheme 2). In doing so, the vacant coordination site left by the hydride is occupied by a second pyrrolyl group to yield *trans*-(κ^P,κ^N-^{Cy}PN)$_2$Ni (**2**). This bis-κ^2-P,N complex is an air-stable compound, which can be more conveniently synthesized by heating $^{Cy}PN^{H}$ with $NiBr_2$ at 90 °C in the presence of Et_3N. Without a carbonyl substrate, **1** dissolved in C_6D_6 slowly loses H_2 at 90 °C (in a sealed NMR tube, ∼90% conversion after 10 d), producing **2** along with a very small amount of $^{Cy}PN^{H}$. The direct H_2 elimination process competes with carbonyl reduction when the reaction is slow (e.g., in the case of reducing $PhCOCH_3$).

Scheme 2. Stoichiometric Reduction of Benzaldehyde and Acetophenone with 1

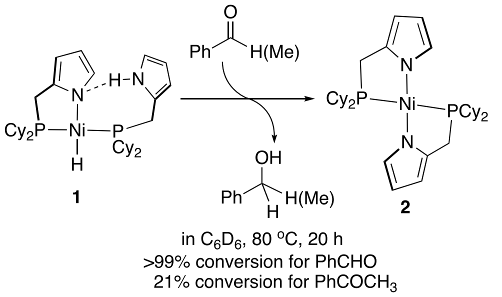

The *trans* geometry in **2** was confirmed by X-ray crystallography (Figure 4).[21] The structure including the key bond distances and angles is similar to that of *trans*-(κ^P,κ^N-^{Ph}PN)$_2$Ni reported by Bochmann,[16b] although in this case the donor atoms (N1, N2, P1, and P2) are more coplanar with nickel (the geometry index τ_4 values[22] are 0.04 and 0.11 for **2** and *trans*-(κ^P,κ^N-^{Ph}PN)$_2$Ni, respectively). As visualized in Scheme 2, the two pyrrolyl rings of **2** are tilted to the opposite directions from the coordination plane by 22.97(6)° and 27.77(6)°.

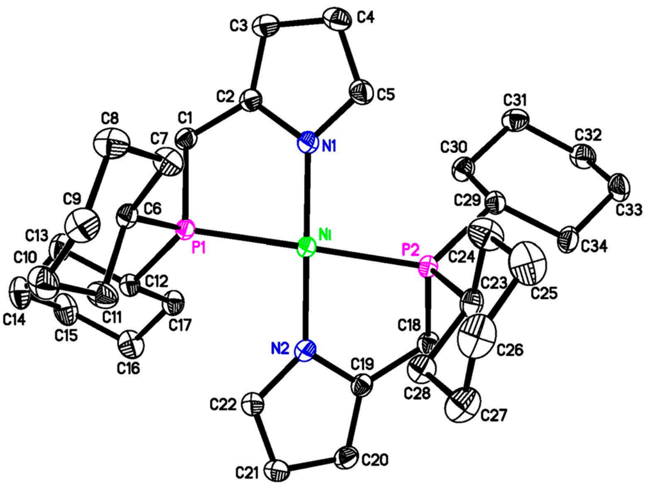

Figure 4. ORTEP drawing of *trans*-(κ^P,κ^N-^{Cy}PN)$_2$Ni (**2**) at the 50% probability level (hydrogen atoms and cocrystallized C_6D_6 molecule are omitted for clarity). Selected interatomic distances (Å) and angles (deg): Ni−N(1) 1.8852(11), Ni−N(2) 1.8921(11), Ni−P(1) 2.2218(4), Ni−P(2) 2.2205(4); N(1)−Ni−P(1) 82.80(3), P(1)−Ni−N(2) 97.24(3), N(2)−Ni−P(2) 81.74(3), P(2)−Ni−N(1) 98.10(3), N(1)−Ni−N(2) 177.07(5), P(1)−Ni−P(2) 177.461(15).

Having demonstrated the capability of **1** to reduce carbonyl substrates stoichiometrically, we went on to study the catalytic hydrogenation reaction. As summarized in Table 1, with a catalyst loading of 5 mol %, a full conversion of benzaldehyde to benzyl alcohol can be accomplished at 100 °C in 20 h under 40 bar H_2 pressure. Under the same conditions except using **2** as the catalyst, only 23% of benzaldehyde was reduced to benzyl alcohol (entry 2), suggesting that the mechanism cannot be simply a H^+/H^- transfer as shown in Scheme 2 followed by H_2 activation with **2** to regenerate the nickel hydride. As a matter of fact, at 100 °C, the bis-κ^2-P,N complex showed no activity toward H_2 (40 bar). Lowering the temperature from 100 to 55 °C shut down the catalytic reduction (entry 3), and adding elemental mercury retarded

Table 1. Hydrogenation of Benzaldehyde and Acetophenone Catalyzed by 1 and 2[a]

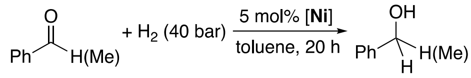

entry	substrate	[Ni]	temp (°C)	conversion (%)
1	PhCHO	**1**	100	100
2	PhCHO	**2**	100	23
3	PhCHO	**1**	55	0
4[b]	PhCHO	**1**	100	37
5[b]	PhCHO	**2**	100	3
6	$PhCOCH_3$	**1**	100	7

[a]Reaction scale: PhCOR (0.16 mmol) and a nickel catalyst (0.008 mmol) mixed with 1 mL of toluene. [b]Hg was added (~400 equiv relative to **1** or **2**).

(though did not completely suppress) the reaction (entry 4). These results provide a strong indication that the catalytic hydrogenation reaction is at least partially promoted by nickel particles, presumably formed via degradation of the metal complexes. The lower catalytic activity observed with **2** can thus be explained by its higher thermal stability against the release of Ni(0), and the activity can be further attenuated by the added elemental mercury (entry 5). As expected, acetophenone is significantly less reactive, and the reaction was found to be marginally catalytic (entry 6).

To test if the hydride complex could react with a nonpolar double bond, a solution of **1** in C_6D_6 was mixed with ethylene gas (1 bar) in a sealed NMR tube. Monitoring the reaction at room temperature by NMR spectroscopy showed dimerization of ethylene to 1-butene followed by alkene isomerization to *cis*/*trans*-2-butene. The amount of higher oligomers was negligible. A transient intermediate was also observed at the beginning of the reaction, giving spectroscopic data (δ_H a multiplet at ~0.45 ppm; δ_P an AB quartet at 41.3 and 17.1 ppm, J_{AB} = 286.8 Hz) consistent with a nickel ethyl complex[5,12a,23] that resulted from ethylene insertion into the Ni−H bond. This species gradually disappeared as the ethylene gas was consumed. It is likely that two consecutive ethylene insertion events produce a nickel *n*-butyl complex, which undergoes *β*-hydrogen elimination rapidly to release 1-butene and regenerate the nickel hydride.[24] The selectivity for 1-butene can however be eroded by the subsequent 2,1-insertion of 1-butene followed by *β*-hydrogen elimination from the internal carbon to yield *cis*/*trans*-2-butene.[25,26] For a quantitative assessment of our catalytic system, hexamethylcyclotrisiloxane was added as an NMR internal standard, and the initial pressure of ethylene was set at 5 bar (Scheme 3). After 18 h, a mixture of 1-butene, *cis*-2-butene, and *trans*-2-butene was obtained with turnover numbers (TONs) of 62, 13, and 6, respectively.

The ability of **1** to catalyze alkene isomerization was independently verified using 4-methyl-1-pentene as the substrate, although the reaction was considerably slower. Under the conditions outlined in Scheme 4, all isomers of 4-methyl-1-pentene resulting from double-bond migration were

Scheme 3. Dimerization of Ethylene Catalyzed by 1

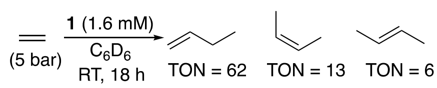

https://doi.org/10.1021/acs.organomet.1c00694
Organometallics 2022, 41, 345−353

Scheme 4. Isomerization of 4-Methyl-1-pentene Catalyzed by 1

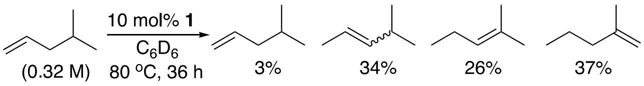

obtained, which roughly represented a thermodynamic mixture.[27] Attempts to intercept the organometallic intermediates with H_2O, $PhCH_2NH_2$, and PhSH failed to produce any heterofunctionalization products. Nevertheless, the addition of D_2O diminished the NH proton resonance of **1** but with no deuterium incorporation into other parts of the molecule or the alkenes. This H/D exchange process did not appear to have any impact on the catalytic isomerization reaction.

Considering that our synthetic route to **1** releases 1,5-COD as a byproduct (Scheme 1), one might have anticipated that the isomerization of 1,5-COD would be affected by the newly generated nickel hydride. This prompted us to monitor the reaction of Ni(1,5-COD)$_2$ with $^{Cy}PN^{H}$ (in C_6D_6) by NMR spectroscopy. Within the time scale of forming **1** (30 min), the extent of isomerization was negligible, and a new nickel species emerged, although the quantity was too small (<5%) to allow definitive characterization. We tentatively assign this species as a C=C bond insertion product. More substantial isomerization was observed when the reaction was conducted at 80 °C for an extended period of time. Analyzing the volatiles following a vacuum distillation showed that 1,5-COD mainly underwent cycloisomerization to yield bicyclo[3.3.0]oct-2-ene, with only a tiny fraction being isomerized to 1,4-COD. The catalytic cycloisomerization of 1,5-COD with presynthesized **1** was optimized by varying the solvent, temperature, and concentration (Table 2). The best result was obtained at

Table 2. Cycloisomerization of 1,5-Cyclooctadiene Catalyzed by 1[a]

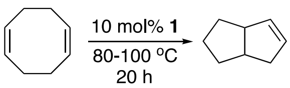

entry	temp (°C)	solvent	volume (mL)	conversion[b] (%)
1	80	toluene	1	34
2	80	EtOH	1	17
3	80	THF	1	49
4	80	benzene	1	54
5	100	toluene	1	50
6	80	benzene	0.5	58
7	100	benzene	0.5	75

[a]Reaction scale: 1,5-cyclooctadiene (0.16 mmol) and **1** (0.016 mmol) mixed with 0.5 or 1 mL of a solvent. [b]Determined by GC.

100 °C in benzene (entry 7), converting 75% of the 1,5-COD to bicyclo[3.3.0]oct-2-ene in 20 h. The process was unaffected by added Hg(0), suggesting that the cycloisomerization reaction is homogeneously catalyzed. Complex **2**, which lacks a hydride moiety available for alkene insertion, proved completely inactive for the cycloisomerization reaction.

The search for additives to further promote the cycloisomerization reaction uncovered that bases such as KO^{t}Bu and Et_3N accelerated the conversion of **1** to the catalytically inactive **2**, which is essentially a thermodynamic sink. Lewis acids including $BH_3{\cdot}THF$ (THF = tetrahydrofuran), $BF_3{\cdot}OEt_2$, and $EtAlCl_2$ quickly decomposed **1** into an intractable mixture. An addition of acetic acid (2 equiv with respect to **1**), however, showed a marked improvement in the catalytic efficiency (Table 3). It resulted in not only an increase in the conversion

Table 3. Catalytic Isomerization of 1,5-Cyclooctadiene with 1 Assisted by Acetic Acid[a]

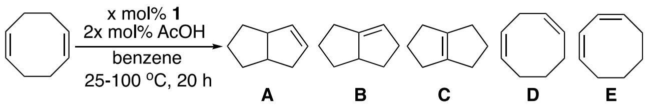

entry	x	temp (°C)	conversion[b] (%)	A/B/C/D/E[b]
1	10	100	100	77.6/1.0/16.8/0/4.6
2	10	50	100	71.1/2.4/24.6/1.6/0.3
3	10	25	71	65.4/19.1/10.2/5.3/0
4	5	50	100	63.1/10.3/22.5/3.8/0.3
5	1	50	95	51.4/22.3/18.5/7.8/0
6[c]	1	50	98.5	66.0/12.5/14.1/7.0/0.4

[a]Reaction scale: 1,5-cyclooctadiene (0.16 mmol), **1** (x mol %), and AcOH ($2x$ mol %) mixed with 0.5 mL of benzene. [b]Determined by GC. [c]Neat conditions (without benzene, 3.3 mmol of 1,5-cyclooctadiene).

of 1,5-COD at lower catalyst loadings and lower temperatures but also the production of other bicyclooctenes (**B** and **C**), which are thermodynamically less stable than bicyclo[3.3.0]-oct-2-ene (**A**).[28] In addition, 2−8% of the 1,5-COD was isomerized to 1,4-COD (**D**) and/or 1,3-COD (**E**). A control experiment with acetic acid only (10 mol %, 50 °C, 24 h) confirmed that the cycloisomerization/isomerization process requires nickel. The reaction could be performed under neat conditions, providing a mixture of isomers **A**−**E** (entry 6). Overall, the product distributions are consistent with the involvement of two parallel catalytic pathways that diverged from the initial insertion product[29] (Scheme 5): the cyclo-

Scheme 5. Proposed Mechanistic Pathways Leading to Products A−E

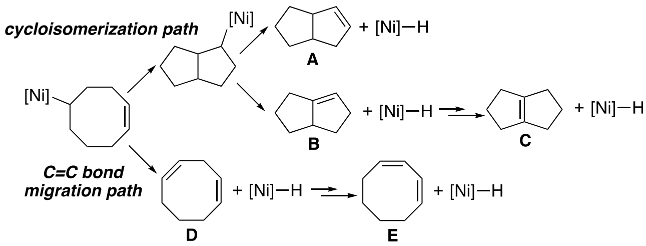

isomerization path (major) and the C=C bond migration path (minor). Compounds **B** and **D** are kinetic products that formed in greater amounts at room temperature (entry 3) or when a low catalyst loading was employed (entry 5). Under the thermodynamic control (entry 1), they were converted to the more stable isomers **A**, **C**, and **E** (relative stability: **A** > **C** > **B** in the bicyclic series;[28] **E** ≫ **D** > 1,5-COD[30]).

Evidently, acetic acid reacts with **1** rapidly to generate a new hydride complex.[31] We initially predicted that protonation would occur to one of the β-carbons of the coordinated pyrrolyl group, analogous to what we observed in the study of an iron hydride supported by a PNP-pincer ligand, *cis*-($\kappa^P,\kappa^N,\kappa^P$-^{Cy}PNP)Fe(CO)$_2$H (^{Cy}PNP = 2,5-bis(dicyclohexylphosphinomethyl)pyrrolyl).[32] To our surprise, the isolated

https://doi.org/10.1021/acs.organomet.1c00694
Organometallics 2022, 41, 345−353

product from the reaction of **1** with acetic acid (>2 equiv) was characterized as *trans*-(κ^P-^{Cy}PN^H)$_2$Ni(OAc)H·HOAc (**3**·HOAc, see Scheme 6) by both X-ray crystallography (Figure 5) and elemental analysis. Instead of protonating the *β*-carbons, acetic acid attacks the pyrrolyl nitrogen, resulting in a net displacement of the pyrrolyl donor by an acetate ligand. The second acetic acid molecule is hydrogen-bonded to this protonation product. These structural modifications to the site *trans* to the hydride causes an elongation of the Ni−P1 bond (from 2.1491(3) Å in **1** to 2.1890(5) Å in **3**·HOAc) and a contraction of the P1−Ni−P2 angle toward the hydride (from 167.340(14)° in **1** to 158.15(2)° in **3**·HOAc).

Scheme 6. Protonation of 1 with Acetic Acid

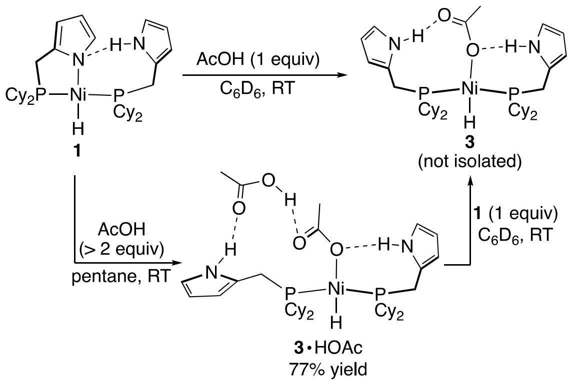

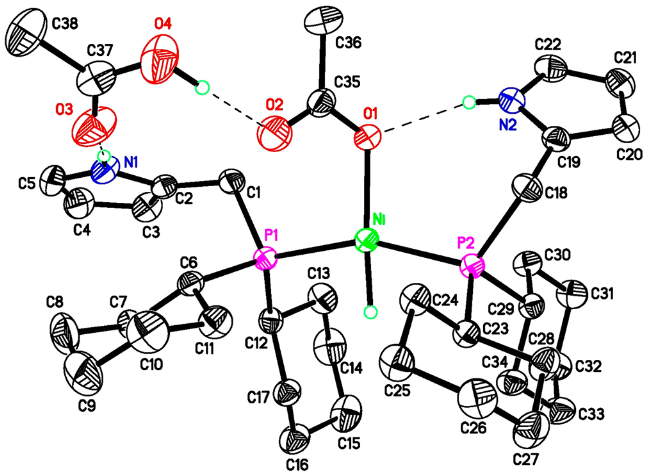

Figure 5. ORTEP drawing of *trans*-(κ^P-^{Cy}PN^H)$_2$Ni(OAc)H·HOAc (**3**·HOAc) at the 50% probability level (cocrystallized C_6D_6 molecule and all hydrogen atoms except those bound to nitrogen, oxygen, and nickel are omitted for clarity). Selected interatomic distances (Å) and angles (deg): Ni−O(1) 1.9398(12), Ni−P(1) 2.1890(5), Ni−P(2) 2.1652(5), Ni−H 1.37(2), C(35)−O(1) 1.278(2), C(35)−O(2) 1.239(2), C(37)−O(3) 1.202(3), C(37)−O(4) 1.302(3), O(1)···N(2) 2.834(2), O(2)···O(4) 2.572(2), O(3)···N(1) 2.898(2); P(1)−Ni−P(2) 158.15(2), O(1)−Ni−P(1) 101.32(4), O(1)−Ni−P(2) 100.53(4).

While the solid-state structure shows different environments around the two ^{Cy}PN^H ligands, **3**·HOAc dissolved in C_6D_6 displays NMR spectra indicative of a more symmetrical molecule. In particular, the hydride resonance was located at −27.19 ppm as a triplet (J_{H-P} = 76.8 Hz), and, in a fully ^{1}H-decoupled spectrum, the phosphorus resonance was found at 27.9 ppm as a singlet. The acetate ligand and the hydrogen-bonded acetic acid must be in fast exchange on the NMR time scale, as suggested by the broadening of the proton and carbon resonances for the CH_3CO_2 groups. Variable-temperature NMR experiments (using toluene-d_8 as the solvent) also showed that these resonances started to decoalesce when the temperature was lowered to ca. −8 °C. The dynamic process may potentially involve a pendulum motion of the hydrogen-bonded network that allows O1 and O3 atoms (referring to Figure 5 for the numbering scheme) to take turns in nickel binding. Alternatively, the acetic acid may quickly dissociate from **3**·HOAc to render the hydride complex symmetrical but would need to reassociate to complete the dynamic process. Samples prepared in situ by adding 1 equiv of acetic acid (or 1 equiv of **3**·HOAc) to **1** gave spectra similar to those for **3**·HOAc, except that the resonances attributed to the CH_3CO_2 groups sharpened and the methyl resonance integrated to 3H instead of 6H. We therefore propose that the product is *trans*-(κ^P-^{Cy}PN^H)$_2$Ni(OAc)H (**3**) without a hydrogen-bonded acetic acid (Scheme 6). In **3**, the NH resonance appeared at 11.54 ppm (cf., 11.20 ppm for the NH and OH resonances in **3**·HOAc), suggesting that hydrogen-bonding interactions with the acetate ligand are still present.

The stability of the hydride moiety toward protonation by acetic acid is noteworthy. In fact, **3**·HOAc can survive in a glacial acetic acid medium. This stands in contrast to our previous study of {κ^P,κ^C,κ^P-2,6-(^{i}Pr$_2$PO)$_2$C$_6$H$_3$}NiH, where carboxylic acids (e.g., PhCO$_2$H) readily protonate the hydride to form a carboxylate complex and H$_2$.[11] Though the hydride is unaffected in this case, one of the Ni−P bonds and the P−Ni−P angle respond to the change from **1** to **3**·HOAc, which likely impacts the lability of the ^{Cy}PN^H ligand and ultimately the distinct activity in the catalytic cycloisomerization of 1,5-COD (Table 3 with in situ-generated **3**·HOAc vs Table 2 with **1**).

Finally, to demonstrate that the cycloisomerization reaction is not limited to cyclic substrates like 1,5-COD, we examined the reaction of 1,5-hexadiene using **1** as the catalyst. With this specific substrate, additives are not needed for full conversion. As shown in Table 4, at room temperature with a catalyst loading of 5 mol %, the reaction reaches completion in 20 h (entry 3), converting 1,5-hexadiene to methylenecyclopentane (**F**) and three different methylcyclopentenes (**G**−**I**). Assuming that 1,5-hexadiene prefers a 1,2-insertion to form [Ni]−(CH$_2$)$_4$CH=CH$_2$ as an intermediate, the subsequent cyclization and *β*-hydrogen elimination steps would generate

Table 4. Cycloisomerization of 1,5-Hexadiene Catalyzed by 1[a]

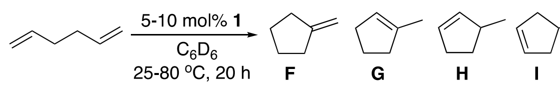

entry	cat loading (mol %)	temp (°C)	conversion (%)[b]	F/G/H/I[b]
1	10	80	100	7.5/47.3/21.1/24.1
2	10	25	100	29.2/33.8/26.2/10.8
3	5	25	100	47.6/36.2/11.0/5.2
4[c]	5	25	100	88.2/9.7/1.9/0.2

[a]Reaction scale: 1,5-hexadiene (0.65 mmol) and **1** (0.033 or 0.065 mmol) mixed in 0.5 mL of C_6D_6. [b]Determined by NMR. [c]Neat conditions (without C_6D_6, 0.98 mmol 1,5-hexadiene)

https://doi.org/10.1021/acs.organomet.1c00694
Organometallics 2022, 41, 345−353

F as the kinetic product.[33] However, a C═C bond migration catalyzed by **1** can convert **F** to the more stable isomers (relative stability: **G** > **I** > **H** > **F**[34]), and an initial 2,1-insertion of 1,5-hexadiene can also lead to **H** and **I** directly (via [Ni]−$CH(CH_3)CH_2CH_2CH{=}CH_2$). Consistent with the analysis, lower temperatures and lower catalyst loadings favor the formation of **F**, and the best selectivity can be achieved under neat conditions (entry 4). The product distribution at 80 °C most likely reflects thermodynamic control (entry 1).

■ CONCLUSION

In summary, we have demonstrated the success in constructing nickel hydride complexes with a pyrrole-derived phosphine ligand. From the coordination chemistry point of view, this ligand is unique in many ways. It can protect the Ni−H bond from degradation and protonation. The pyrrole N−H bond is cleavable, as shown in the synthesis of (κ^P-$^{Cy}PN^H$)(κ^P,κ^N-^{Cy}PN)NiH (via N−H oxidative addition to Ni(1,5-COD)$_2$) and the reduction of carbonyl substrates (via H^+ transfer). The NH functionality is also restorable through the addition of acetic acid, even when the hydride moiety is present. In principle, these properties can be capitalized on in the development of catalytic reactions in an acidic medium that involves a metal hydride. The nickel system presented herein is, however, hindered by the formation of *trans*-(κ^P,κ^N-^{Cy}PN)$_2$Ni, which behaves as a thermodynamic sink. Nevertheless, (κ^P-$^{Cy}PN^H$)(κ^P,κ^N-^{Cy}PN)NiH exhibits reactivity that is unavailable with the related pincer-ligated nickel hydride complexes such as {κ^P,κ^C,κ^P-2,6-$(R_2PO)_2C_6H_3$}NiH. This includes the ability to catalyze ethylene dimerization, isomerization of alkenes, and cycloisomerization of dienes, likely enabled by the more facile ligand dissociation. Our future efforts will be devoted to other metal systems where reactivity might be less dictated by the coordination geometry.

■ EXPERIMENTAL SECTION

General Methods. All metal complexes described in this paper were prepared under an argon atmosphere using standard glovebox and Schlenk techniques. Benzene-d_6 was dried over sodium-benzophenone and distilled under an argon atmosphere. Ethanol was dried over 3 Å molecular sieves and then deoxygenated by bubbling argon through it for 10 min. Other dry and oxygen-free solvents used for synthesis, workup, and catalytic studies (pentane, toluene, and THF) were collected from an Innovative Technology solvent purification system. 2-(Dimethylamino)methyl-1*H*-pyrrole was prepared according to a literature procedure.[17] Chemical shift values in ^{1}H and ^{13}C{^{1}H} NMR spectra were referenced internally to the residual solvent resonances. ^{31}P{^{1}H} spectra were referenced externally to 85% H_3PO_4 (0 ppm). Infrared spectra were recorded on a PerkinElmer Spectrum Two FT-IR spectrometer equipped with a smart orbit diamond attenuated total reflectance (ATR) accessory.

Synthesis of $^{Cy}PN^H$. Under an argon atmosphere, a 25 mL oven-dried Schlenk flask equipped with a stir bar was charged with 2-(dimethylamino)methyl-1*H*-pyrrole (3.0 g, 24.2 mmol) and dicyclohexylphosphine (5.3 g, 26.7 mmol). The resulting slurry was heated to 130 °C to give a clear solution, which was stirred at this temperature for 18 h. The solution was then cooled to 80 °C, and vacuum was applied to remove the volatiles. The resulting off-white waxy solid was washed with 10 mL of pentane, followed by drying under vacuum to afford the desired product as a white powder (5.44 g, 81% yield). ^{1}H, ^{13}C{^{1}H}, and ^{31}P{^{1}H} NMR spectra match those previously reported.[16b] ^{1}H NMR (400 MHz, $CDCl_3$, δ): 8.28 (br, pyrrole N*H*, 1H), 6.66 (s, pyrrole C*H*, 1H), 6.09 (s, pyrrole C*H*, 1H), 5.92 (s, pyrrole C*H*, 1H), 2.81 (s, PC*H*$_2$, 2H), 1.84−1.02 (m, cyclohexyl C*H* and C*H*$_2$, 22H). ^{13}C{^{1}H} NMR (101 MHz, $CDCl_3$, δ): 129.2 (d, J_{C-P} = 8.5 Hz, pyrrole *C*), 116.3 (s, pyrrole *C*H), 108.4 (s, pyrrole *C*H), 106.3 (d, J_{C-P} = 4.3 Hz, pyrrole *C*H), 33.4 (d, J_{C-P} = 13.1 Hz, P*C*H), 29.9 (d, J = 13.0 Hz, cyclohexyl *C*H$_2$), 28.9 (d, J_{C-P} = 8.0 Hz, cyclohexyl *C*H$_2$), 27.5 (d, J_{C-P} = 10.9 Hz, cyclohexyl *C*H$_2$), 27.3 (d, J_{C-P} = 7.8 Hz, cyclohexyl *C*H$_2$), 26.6 (s, cyclohexyl *C*H$_2$), 20.5 (d, J_{C-P} = 18.5 Hz, P*C*H$_2$). ^{31}P{^{1}H} NMR (162 MHz, $CDCl_3$, δ): −6.0 (s). Selected ATR-IR data (neat, cm^{-1}): 3250 (ν_{N-H}), 2920, 2846, 1566, 1444.

Synthesis of (κ^P-$^{Cy}PN^H$)(κ^P,κ^N-^{Cy}PN)NiH (1). Under an argon atmosphere, a 100 mL oven-dried Schlenk flask equipped with a stir bar was charged with $^{Cy}PN^H$ (1.09 g, 3.93 mmol) and 10 mL of toluene. A solution of Ni(1,5-COD)$_2$ (540 mg, 1.96 mmol) in 50 mL of toluene was added dropwise (over 15 min), resulting in an immediate color change from colorless to red and then to dark brown. After the addition, the mixture was stirred for another 15 min, and then the volatiles were removed under vacuum. The resulting black oil was treated with 30 mL of pentane and filtered to remove a trace of black solid. The pentane solution was seeded with a crystal of the product (or scratched repeatedly the first time) to initiate a yellow precipitate. The solid was collected by filtration, washed with EtOH (10 mL × 2), and dried under vacuum to afford the desired product as a finely divided yellow powder (525 mg, 44% yield). X-ray quality crystals were grown from a saturated pentane solution kept at −27 °C. ^{1}H NMR (400 MHz, C_6D_6, δ): 9.31 (s, pyrrole N*H*, 1H), 7.07 (s, pyrrole C*H*, 1H), 6.88 (s, pyrrole C*H*, 1H), 6.65 (d, J = 2.2 Hz, pyrrole C*H*, 1H), 6.37 (s, pyrrole C*H*, 1H), 6.18 (q, J = 2.6 Hz, pyrrole C*H*, 1H), 6.06 (s, pyrrole C*H*, 1H), 3.07 (dd, J = 7.4 and 2.6 Hz, PC*H*$_2$, 2H), 2.96 (d, J = 10.0 Hz, PC*H*$_2$, 2H), 2.10−2.00 (m, cyclohexyl C*H*, 2H), 1.97−1.88 (m, cyclohexyl C*H*, 2H), 1.74−0.93 (m, cyclohexyl C*H*$_2$, 40H), −20.78 (dd, J_{H-P} = 73.8 and 69.4 Hz, Ni*H*, 1H). ^{13}C{^{1}H} NMR (101 MHz, C_6D_6, δ): 140.8 (dd, J_{C-P} = 10.0 and 4.8 Hz, pyrrole *C*), 129.3 (s, pyrrole *C*), 125.3 (d, J_{C-P} = 1.9 Hz, pyrrole *C*H), 117.9 (s, pyrrole *C*H), 111.7 (s, pyrrole *C*H), 107.85 (d, J_{C-P} = 4.3 Hz, pyrrole *C*H), 107.84 (s, pyrrole *C*H), 104.0 (d, J_{C-P} = 10.5 Hz, pyrrole *C*H), 37.3 (d, J_{C-P} = 24.5 Hz, P*C*H), 34.2 (d, J_{C-P} = 24.8 Hz, P*C*H), 29.6 (d, J_{C-P} = 3.1 Hz, cyclohexyl *C*H$_2$), 29.4 (d, J_{C-P} = 2.7 Hz, cyclohexyl *C*H$_2$), 28.6 (s, cyclohexyl *C*H$_2$), 27.7 (d, J_{C-P} = 11.6 Hz, cyclohexyl *C*H$_2$), 27.4 (d, J_{C-P} = 9.9 Hz, cyclohexyl *C*H$_2$), 27.1 (d, J_{C-P} = 8.9 Hz, cyclohexyl *C*H$_2$), 27.0 (d, J_{C-P} = 6.5 Hz, cyclohexyl *C*H$_2$), 26.7 (s, cyclohexyl *C*H$_2$), 26.5 (s, cyclohexyl *C*H$_2$), 23.3 (d, J_{C-P} = 16.3 Hz, P*C*H$_2$), 21.1 (dd, J_{C-P} = 8.6 and 3.7 Hz, P*C*H$_2$). ^{31}P{^{1}H} NMR (162 MHz, C_6D_6, δ): 62.8 (AB, J_{AB} = 251.2 Hz, 1P), 29.2 (AB, J_{AB} = 251.2 Hz, 1P). Selected ATR-IR data (solid, cm^{-1}): 3316 (ν_{N-H}), 2917, 2846, 1912 (ν_{Ni-H}), 1447. Anal. Calcd for $C_{34}H_{56}N_2P_2Ni$: C, 66.57; H, 9.20; N, 4.57. Found: C, 66.44; H, 9.25; N, 4.54%.

Synthesis of *trans*-(κ^P,κ^N-^{Cy}PN)$_2$Ni (2). Under an argon atmosphere, a 25 mL oven-dried Schlenk flask equipped with a stir bar was charged with toluene (10 mL), $^{Cy}PN^H$ (200 mg, 0.72 mmol), $NiBr_2$ (83 mg, 0.38 mmol), and Et_3N (151 μL, 1.08 mmol). The resulting slurry was stirred at 90 °C for 16 h, giving a dark red mixture. The insoluble material was filtered off, and the filtrate was concentrated under vacuum to yield a red oil, which was triturated with 5 mL of pentane. The resulting solid was collected by filtration and dried under vacuum to afford the desired product as a light red powder (109 mg, 50% yield). This compound (in both solution and solid forms) can be handled in air without noticeable degradation. X-ray quality crystals were grown by layering a C_6D_6 solution with pentane or by evaporating a toluene solution. ^{1}H NMR (400 MHz, C_6D_6, δ): 6.62 (t, J = 2.7 Hz, pyrrole C*H*, 2H), 6.48 (br, pyrrole C*H*, 2H), 6.35 (d, J = 3.1 Hz, pyrrole C*H*, 2H), 2.81 (t, J = 3.6 Hz, PC*H*$_2$, 4H), 2.19−0.92 (m, cyclohexyl C*H* and C*H*$_2$, 44H). ^{13}C{^{1}H} NMR (101 MHz, C_6D_6, δ): 138.8 (t, J = 5.3 Hz, pyrrole *C*), 130.7 (t, J = 4.2 Hz, pyrrole *C*H), 111.4 (s, pyrrole *C*H), 103.7 (t, J = 4.2 Hz, pyrrole *C*H), 34.6 (t, J = 9.4 Hz, P*C*H), 29.5 (s, cyclohexyl *C*H$_2$), 28.5 (s, cyclohexyl *C*H$_2$), 27.6 (t, J = 6.5 Hz, cyclohexyl *C*H$_2$), 27.2 (t, J = 4.4 Hz, cyclohexyl *C*H$_2$), 26.3 (s, cyclohexyl *C*H$_2$), 22.4 (t, J = 11.4 Hz, P*C*H$_2$). ^{31}P{^{1}H} NMR (162 MHz, C_6D_6, δ): 47.7 (s). Selected ATR-IR data (solid, cm^{-1}): 2928, 2845, 1447. Anal. Calcd for

https://doi.org/10.1021/acs.organomet.1c00694
Organometallics 2022, 41, 345−353

$C_{34}H_{54}N_2P_2Ni$: C, 66.79; H, 8.90; N, 4.58. Found: C, 67.06; H, 9.00; N, 4.67%.

Synthesis of *trans*-(κ^P-$^{Cy}PN^H$)$_2$Ni(OAc)H·HOAc (3·HOAc). Under an argon atmosphere, a scintillation vial was charged with **1** (50 mg, 0.082 mmol) suspended in 5 mL of pentane. Acetic acid (17 μL, 0.30 mmol) was added, resulting in an immediate dissolution of the solid and formation of a dark yellow solution. The vial was kept in a −27 °C freezer for 18 h, at which point dark yellow crystals were observed. The liquid was decanted, and the crystals were left under a stream of argon to yield an analytically pure sample (46 mg, 77% yield). X-ray quality crystals were grown from a solution of benzene−pentane (~1:4) kept at −27 °C. ^{1}H NMR (400 MHz, C_6D_6, δ): 11.20 (br, N*H* and O*H*, 3H), 6.94 (s, pyrrole C*H*, 2H), 6.36 (s, pyrrole C*H*, 2H), 6.06 (s, pyrrole C*H*, 2H), 2.87 (s, PCH_2, 4H), 2.01−1.81 (m, PC*H* and CH_3CO$_2$, 10H), 1.75−1.05 (m, cyclohexyl CH_2, 40H), −27.19 (t, J_{H-P} = 76.8 Hz, Ni*H*, 1H). ^{13}C{^{1}H} NMR (101 MHz, C_6D_6, δ): 177.1−176.5 (m, CH_3CO_2), 124.9 (s, pyrrole *C*), 117.7 (s, pyrrole *C*H), 108.5 (s, pyrrole *C*H), 108.0 (s, pyrrole *C*H), 36.1 (t, J_{C-P} = 12.5 Hz, P*C*H), 29.3 (s, cyclohexyl *C*H$_2$), 28.7 (s, cyclohexyl *C*H$_2$), 27.6 (t, J_{C-P} = 5.5 Hz, cyclohexyl *C*H$_2$), 27.5 (t, J_{C-P} = 4.7 Hz, cyclohexyl *C*H$_2$), 26.6 (s, cyclohexyl *C*H$_2$), 22.6 (br, *C*H$_3$CO$_2$), 20.7 (t, J_{C-P} = 6.0 Hz, P*C*H$_2$). ^{31}P{^{1}H} NMR (162 MHz, C_6D_6, δ): 27.9 (s). Selected ATR-IR data (solid, cm^{-1}): 3348 (ν_{N-H} or ν_{O-H}), 3301 (ν_{N-H} or ν_{O-H}), 2931, 2847, 1960 (ν_{Ni-H}), 1694 (ν_{OCO}), 1445, 1402. Anal. Calcd for $C_{38}H_{64}N_2O_4P_2Ni$: C, 62.22; H, 8.79; N, 3.82. Found: C, 62.59; H, 8.79; N, 3.99%.

Catalytic Dimerization of Ethylene. Under an argon atmosphere, to a Wilmad Quick Pressure Valve NMR tube (medium wall, rated for 150 psi, part No. 524-QPV-7) was added **1** (0.5 mg, 0.8 μmol), C_6D_6 (0.5 mL), and hexamethylcyclotrisiloxane (0.5 mg, 2.2 μmol, internal standard). The NMR tube was degassed via three freeze−pump−thaw cycles and then charged with ethylene gas (5 bar, measured at room temperature). The tube was secured to a device that allowed the solution to be continuously mixed with the gas. After this was allowed to react at room temperature for 18 h, the diagnostic ^{1}H NMR resonances (verified by authentic samples and matched with the literature data[35]) were compared to that of the internal standard to determine the TONs for the three oligomers: 1-butene (TON = 62), *cis*-2-butene (TON = 13), and *trans*-2-butene (TON = 6).

Catalytic Cycloisomerization/Isomerization of 1,5-Cyclooctadiene. Under an argon atmosphere to a 2 mL Schlenk tube equipped with a stir bar was added **1** (20 mg, 33 μmol), acetic acid (3.7 μL, 65 μmol), and 1,5-COD (400 μL, 3.3 mmol). The tube was sealed and heated to the desired temperature with stirring for 20 h. All volatile components were collected via vacuum distillation, which yielded a colorless liquid (293 mg, 83% yield, calculated in one run). The product composition was determined by NMR and gas chromatography−mass spectrometry (GC-MS). The ^{1}H and ^{13}C{^{1}H} NMR spectra for the individual isomers match those previously reported (**A**: *cis*-bicyclo[3.3.0]oct-2-ene,[36] **B**: bicyclo[3.3.0]oct-1(2)-ene,[37] **C**: bicyclo[3.3.0]oct-1(5)-ene,[36c,37,38] **D**: 1,4-cyclooctadiene,[39] **E**: 1,3-cyclooctadiene[39]).

Catalytic Cycloisomerization of 1,5-Hexadiene. Under an argon atmosphere, to a 2 mL Schlenk tube was added **1** (30 mg, 49 μmol) and 1,5-hexadiene (116 μL, 0.98 mmol). The tube was sealed and heated to the desired temperature with stirring for 20 h. All volatile components were collected via vacuum distillation, which yielded a colorless liquid (49 mg, 61% yield, calculated in one run). The product distribution was determined by diagnostic ^{1}H NMR resonances. The ^{1}H and ^{13}C{^{1}H} NMR spectra for the individual isomers match those previously reported (**F**: methylenecyclopentane,[40] **G**: 1-methylcyclopentene,[41] **H**: 3-methylcyclopentene,[42] **I**: 4-methylcyclopentene[43]).

X-ray Structure Determinations. Crystal data collection and refinement parameters are provided in the Supporting Information. Details on how single crystals were obtained are described in the corresponding synthesis and characterization subsections. Intensity data were collected at 150 K on a Bruker D8 Venture Photon-II diffractometer with Cu Kα radiation, λ = 1.541 78 Å (for **1**), or with Mo Kα radiation, λ = 0.710 73 Å (for other structures). Data collection frames were measured in a shutterless mode. The data frames were processed using the program SAINT. The data were corrected for decay, Lorentz, and polarization effects as well as absorption and beam corrections based on the multiscan technique. The structures were solved by a combination of direct methods and the difference Fourier technique as implemented in the SHELX suite of programs and refined by full-matrix least-squares on F^2. Non-hydrogen atoms were refined with anisotropic displacement parameters. The hydrogen atoms bound to nickel or involved in hydrogen-bonding interactions were located directly from the difference map, and the coordinates were refined. The remaining hydrogen atoms were calculated and treated with a riding model. Compound **2** cocrystallizes with C_6D_6 or toluene; in the latter case, the toluene molecule is disordered and was refined with a two-component disorder model (occupancy set at 0.5). Compound **3** cocrystallizes with both CH_3CO_2H and C_6D_6. Additional crystallographic information is available in the Supporting Information.

■ ASSOCIATED CONTENT

Supporting Information

The Supporting Information is available free of charge at https://pubs.acs.org/doi/10.1021/acs.organomet.1c00694.

NMR and IR spectra of the $^{Cy}PN^H$ ligand and its nickel complexes (**1**, **2**, **3**·HOAc, and **3**); additional X-ray crystallographic information (PDF)

Accession Codes

CCDC 2128622−2128625 contain the supplementary crystallographic data for this paper. These data can be obtained free of charge via www.ccdc.cam.ac.uk/data_request/cif, or by emailing data_request@ccdc.cam.ac.uk, or by contacting The Cambridge Crystallographic Data Centre, 12 Union Road, Cambridge CB2 1EZ, UK; fax: + 44 1223 336033.

■ AUTHOR INFORMATION

Corresponding Author

Hairong Guan − *Department of Chemistry, University of Cincinnati, Cincinnati, Ohio 45221-0172, United States*; orcid.org/0000-0002-4858-3159; Email: hairong.guan@uc.edu

Authors

Joel D. Collett − *Department of Chemistry, University of Cincinnati, Cincinnati, Ohio 45221-0172, United States*

Jeanette A. Krause − *Department of Chemistry, University of Cincinnati, Cincinnati, Ohio 45221-0172, United States*

Complete contact information is available at: https://pubs.acs.org/10.1021/acs.organomet.1c00694

Notes

The authors declare no competing financial interest.

■ ACKNOWLEDGMENTS

We thank the NSF Chemical Catalysis Program (CHE-1800151 and CHE-2102192) for support of this research. Crystallographic data were collected on a Bruker D8 Venture diffractometer that was funded by an NSF MRI grant (CHE-1625737).

■ REFERENCES

(1) Eberhardt, N. A.; Guan, H. Nickel Hydride Complexes. *Chem. Rev.* **2016**, *116*, 8373−8426.

(2) Chakraborty, S.; Bhattacharya, P.; Dai, H.; Guan, H. Nickel and Iron Pincer Complexes as Catalysts for the Reduction of Carbonyl Compounds. *Acc. Chem. Res.* **2015**, *48*, 1995−2003.

(3) Chakraborty, S.; Krause, J. A.; Guan, H. Hydrosilylation of Aldehydes and Ketones Catalyzed by Nickel PCP-Pincer Hydride Complexes. *Organometallics* **2009**, *28*, 582−586.
(4) Grüger, N.; Wadepohl, H.; Gade, L. H. A Readily Accessible PNP Pincer Ligand with a Pyrrole Backbone and Its $Ni^{I/II}$ Chemistry. *Dalton Trans.* **2012**, *41*, 14028−14030.
(5) Venkanna, G. T.; Tammineni, S.; Arman, H. D.; Tonzetich, Z. J. Synthesis, Characterization, and Catalytic Activity of Nickel(II) Alkyl Complexes Supported by Pyrrole-Diphosphine Ligands. *Organometallics* **2013**, *32*, 4656−4663.
(6) Kreye, M.; Freytag, M.; Jones, P. G.; Williard, P. G.; Bernskoetter, W. H.; Walter, M. D. Homolytic H_2 Cleavage by a Mercury-Bridged Ni(I) Pincer Complex [{(PNP)Ni}$_2${μ-Hg}]. *Chem. Commun.* **2015**, *51*, 2946−2949.
(7) (a) Chakraborty, S.; Patel, Y. J.; Krause, J. A.; Guan, H. A Robust Nickel Catalyst for Cyanomethylation of Aldehydes: Activation of Acetonitrile under Base-Free Conditions. *Angew. Chem., Int. Ed.* **2013**, *52*, 7523−7526. (b) Martínez-Prieto, L. M.; Ávila, E.; Palma, P.; Álvarez, E.; Cámpora, J. β-Hydrogen Elimination Reactions of Nickel and Palladium Methoxides Stabilised by PCP Pincer Ligands. *Chem. Eur. J.* **2015**, *21*, 9833−9849.
(8) (a) Chakraborty, S.; Zhang, J.; Krause, J. A.; Guan, H. An Efficient Nickel Catalyst for the Reduction of Carbon Dioxide with a Borane. *J. Am. Chem. Soc.* **2010**, *132*, 8872−8873. (b) Schmeier, T. J.; Hazari, N.; Incarvito, C. D.; Raskatov, J. A. Exploring the Reactions of CO_2 with PCP Supported Nickel Complexes. *Chem. Commun.* **2011**, *47*, 1824−1826. (c) Chakraborty, S.; Patel, Y. J.; Krause, J. A.; Guan, H. Catalytic Properties of Nickel Bis(phosphinite) Pincer Complexes in the Reduction of CO_2 to Methanol Derivatives. *Polyhedron* **2012**, *32*, 30−34. (d) Suh, H.-W.; Schmeier, T. J.; Hazari, N.; Kemp, R. A.; Takase, M. K. Experimental and Computational Studies of the Reaction of Carbon Dioxide with Pincer-Supported Nickel and Palladium Hydrides. *Organometallics* **2012**, *31*, 8225−8236. (e) Jonasson, K. J.; Wendt, O. F. Synthesis and Characterization of a Family of POCOP Pincer Complexes with Nickel: Reactivity Towards CO_2 and Phenylacetylene. *Chem. Eur. J.* **2014**, *20*, 11894−11902. (f) Murugesan, S.; Stöger, B.; Weil, M.; Veiros, L. F.; Kirchner, K. Synthesis, Structure, and Reactivity of Co(II) and Ni(II) PCP Pincer Borohydride Complexes. *Organometallics* **2015**, *34*, 1364−1372. (g) Wellala, N. P. N.; Dong, H. T.; Krause, J. A.; Guan, H. Janus POCOP Pincer Complexes of Nickel. *Organometallics* **2018**, *37*, 4031−4039. (h) Heimann, J. E.; Bernskoetter, W. H.; Hazari, N.; Mayer, J. M. Acceleration of CO_2 Insertion into Metal Hydrides: Ligand, Lewis Acid, and Solvent Effects on Reaction Kinetics. *Chem. Sci.* **2018**, *9*, 6629−6638.
(9) Ma, Q.-Q.; Liu, T.; Adhikary, A.; Zhang, J.; Krause, J. A.; Guan, H. Using CS_2 to Probe the Mechanistic Details of Decarboxylation of Bis(phosphinite)-Ligated Nickel Pincer Formate Complexes. *Organometallics* **2016**, *35*, 4077−4082.
(10) (a) Huang, F.; Zhang, C.; Jiang, J.; Wang, Z.-X.; Guan, H. How Does the Nickel Pincer Complex Catalyze the Conversion of CO_2 to a Methanol Derivatives? A Computational Mechanistic Study. *Inorg. Chem.* **2011**, *50*, 3816−3825. (b) Chakraborty, S.; Zhang, J.; Patel, Y. J.; Krause, J. A.; Guan, H. Pincer-Ligated Nickel Hydridoborate Complexes: the Dormant Species in Catalytic Reduction of Carbon Dioxide with Boranes. *Inorg. Chem.* **2013**, *52*, 37−47. (c) Espinosa, M. R.; Charboneau, D. J.; Garcia de Oliveira, A.; Hazari, N. Controlling Selectivity in the Hydroboration of Carbon Dioxide to the Formic Acid, Formaldehyde, and Methanol Oxidation Levels. *ACS Catal.* **2019**, *9*, 301−314. (d) Ma, N.; Tu, C.; Xu, Q.; Guo, W.; Zhang, J.; Zhang, G. Computational Study on the Mechanism of Hydroboration of CO_2 Catalysed by POCOP Pincer Nickel Thiolate Complexes: Concerted Catalysis and Hydride Transfer by a Shuttle. *Dalton Trans.* **2021**, *50*, 2903−2914.
(11) Eberhardt, N. A.; Wellala, N. P. N.; Li, Y.; Krause, J. A.; Guan, H. Dehydrogenative Coupling of Aldehydes with Alcohols Catalyzed by a Nickel Hydride Complex. *Organometallics* **2019**, *38*, 1468−1478.
(12) (a) Müller, U.; Keim, W.; Krüger, C.; Betz, P. [{$Ph_2PCH_2C(CF_3)_2O$}NiH(PCy_3)]: Support for a Nickel Hydride Mechanism in Ethene Oligomerization. *Angew. Chem., Int. Ed. Engl.* **1989**, *28*, 1011−1013. (b) Jenkins, J. C.; Brookhart, M. A Mechanistic Investigation of the Polymerization of Ethylene Catalyzed by Neutral Ni(II) Complexes Derived from Bulky Anilinotropone Ligands. *J. Am. Chem. Soc.* **2004**, *126*, 5827−5842. (c) Chen, M.-T.; Lee, W.-Y.; Tsai, T.-L.; Liang, L.-C. Nickel(II) Complexes Containing Bidentate Diarylamido Phosphine Chelates: Kumada Couplings Kinetically Preferred to β-Hydrogen Elimination. *Organometallics* **2014**, *33*, 5852−5862.
(13) (a) Vabre, B.; Deschamps, F.; Zargarian, D. Ortho Derivatization of Phenols through C−H Nickelation: Synthesis, Characterization, and Reactivities of Ortho-Nickelated Phosphinite Complexes. *Organometallics* **2014**, *33*, 6623−6632. (b) Mangin, L. P.; Zargarian, D. C−H Nickellation of Phenol-Derived Phosphinites: Regioselectivity and Structures of Cyclonickellated Complexes. *Dalton Trans.* **2017**, *46*, 16159−16170. (c) Mangin, L. P.; Zargarian, D. C−H Nickelation of Aryl Phosphinites: Mechanistic Aspects. *Organometallics* **2019**, *38*, 1479−1492. (d) Mangin, L. P.; Zargarian, D. C−H Nickelation of Naphthyl Phosphinites: Electronic and Steric Limitations, Regioselectivity, and Tandem C−P Functionalization. *Organometallics* **2019**, *38*, 4687−4700.
(14) Thompson, C. V.; Tonzetich, Z. J. Pincer Ligands Incorporating Pyrrolyl Units: Versatile Platforms for Organometallic Chemistry and Catalysis. *Adv. Organomet. Chem.* **2020**, *74*, 153−240.
(15) Hart, J. S.; Nichol, G. S.; Love, J. B. Directed Secondary Interactions in Transition Metal Complexes of Tripodal Pyrrole Imine and Amide Ligands. *Dalton Trans.* **2012**, *41*, 5785−5788.
(16) (a) Broomfield, L. M.; Wright, J. A.; Bochmann, M. Synthesis, Structures and Reactivity of 2-Phosphorylmethyl-1*H*-pyrrolato Complexes of Titanium, Yttrium and Zinc. *Dalton Trans.* **2009**, 8269−8279. (b) Broomfield, L. M.; Boschert, D.; Wright, J. A.; Hughes, D. L.; Bochmann, M. Synthesis of Neutral and Zwitterionic Phosphinomethylpyrrolato Complexes of Nickel. *J. Organomet. Chem.* **2009**, *694*, 4084−4089.
(17) Herz, W.; Dittmer, K.; Cristol, S. J. The Preparation of Some Monosubstituted Derivatives of Pyrrole by the Mannich Reaction. *J. Am. Chem. Soc.* **1947**, *69*, 1698−1700.
(18) (a) Kumar, S.; Mani, G.; Mondal, S.; Chattaraj, P. K. Pyrrole-Based New Diphosphines: Pd and Ni Complexes Bearing the PNP Pincer Ligand. *Inorg. Chem.* **2012**, *51*, 12527−12539. (b) Kessler, J. A.; Iluc, V. M. Ag(I) and Tl(I) Precursors as Transfer Agents of a Pyrrole-Based Pincer Ligand to Late Transition Metals. *Inorg. Chem.* **2014**, *53*, 12360−12371. (c) Venkanna, G. T.; Arman, H. D.; Tonzetich, Z. J. Catalytic C−S Cross-Coupling Reactions Employing Ni Complexes of Pyrrole-Based Pincer Ligands. *ACS Catal.* **2014**, *4*, 2941−2950. (d) Levine, D. S.; Tilley, T. D.; Andersen, R. A. C−H Bond Activations by Monoanionic, PNP-Supported Scandium Dialkyl Complexes. *Organometallics* **2015**, *34*, 4647−4655.
(19) The structural parameters determined for N1···H−N2 ($d_{N1\cdots H}$ = 2.59(2) Å, $d_{N1\cdots N2}$ = 3.322(1) Å, $\angle_{N1\cdots H-N2}$ = 151(2)°) allows N1···H to qualify as a weak hydrogen bond. For structural criteria for weak hydrogen bonds, see: Desiraju, G. R.; Steiner, T. *The Weak Hydrogen Bond in Structural Chemistry and Biology. IUCr Monographs on Crystallography;* Oxford University Press: Oxford, England, 1999; Vol. 9.
(20) Khusnutdinova, J. R.; Milstein, D. Metal−Ligand Cooperation. *Angew. Chem., Int. Ed.* **2015**, *54*, 12236−12273.
(21) Figure 4 shows the structure of **2** solved using single crystals grown from C_6D_6-pentane. Single crystals were also grown from a toluene solution. The results are provided in the Supporting Information.
(22) Yang, L.; Powell, D. R.; Houser, R. P. Structural Variation in Copper(I) Complexes with Pyridylmethylamide Ligands: Structural Analysis with a New Four-Coordinate Geometry Index, τ_4. *Dalton Trans.* **2007**, 955−964.
(23) (a) Liang, L.-C.; Chien, P.-S.; Lin, J.-M.; Huang, M.-H.; Huang, Y.-L.; Liao, J.-H. Amido Pincer Complexes of Ni(II): Synthesis, Structure, and Reactivity. *Organometallics* **2006**, *25*, 1399−1411. (b) Pandarus, V.; Zargarian, D. New Pincer-Type Diphosphinito

https://doi.org/10.1021/acs.organomet.1c00694
Organometallics 2022, 41, 345−353

(POCOP) Complexes of Nickel. *Organometallics* **2007**, *26*, 4321−4334.

(24) Pillai, S. M.; Ravindranathan, M.; Sivaram, S. Dimerization of Ethylene and Propylene Catalyzed by Transition-Metal Complexes. *Chem. Rev.* **1986**, *86*, 353−399.

(25) Kuhn, P.; Sémeril, D.; Matt, D.; Chetcuti, M. J.; Lutz, P. Structure-Reactivity Relationships in SHOP-Type Complexes: Tunable Catalysts for the Oligomerisation and Polymerisation of Ethylene. *Dalton Trans.* **2007**, 515−528.

(26) We cannot rule out the possibility of H· transfer from nickel to 1-butene followed by a hydrogen atom abstraction with the resulting radicals.

(27) The ratios of these isomers were unchanged when the reaction time was extended to 72 h, at which point **1** remained in the solution.

(28) Rogers, D. W.; McLafferty, F. J. G3(MP2) Calculations of Enthalpies of Hydrogenation, Isomerization, and Formation of Bi- and Tricyclic C_8 and C_{10} Hydrocarbons. The Bicyclo[3.3.0]octenes and Triquinacenes. *J. Phys. Chem. A* **2000**, *104*, 9356−9361.

(29) The initial insertion product may or may not have the remaining C═C bond coordinated to nickel.

(30) Taskinen, E.; Nummelin, K. Relative Thermodynamic Stabilities of the Isomeric Cyclooctadienes. *Acta Chem. Scand., Ser. B* **1985**, *39b*, 791−792.

(31) Similarly, HCO_2H and CF_3CO_2H react with **1** to yield new nickel hydrides, although we have not made efforts to isolate and fully characterize these hydride complexes.

(32) Collett, J. D.; Ransohoff, R. W.; Krause, J. A.; Guan, H. An Iron-Hydrogen Bond Resistant to Protonation and Oxidation. *Z. Anorg. Allg. Chem.* **2021**, *647*, 1449−1454.

(33) We cannot rule out the possibility of H· transfer from nickel to 1,5-hexadiene followed by a radical cyclization and then hydrogen atom abstraction by the metalloradical. For a representative catalytic system, see: Li, G.; Kuo, J. L.; Han, A.; Abuyuan, J. M.; Young, L. C.; Norton, J. R.; Palmer, J. H. Radical Isomerization and Cycloisomerization Initiated by H· Transfer. *J. Am. Chem. Soc.* **2016**, *138*, 7698−7704.

(34) Yursha, I. A.; Kabo, G. Ya Thermodynamics of the Isomerisation of Methylcyclopentines. *Russ. J. Phys. Chem.* **1975**, *49*, 765−766.

(35) Lumbreras, E., Jr.; Sisler, E. M.; Shelby, Q. D. Synthesis, X-ray Crystal Structure, and Reactivity of $Pd_2(\mu\text{-dotpm})_2$ (dotpm = bis(di-*ortho*-tolylphosphino)methane). *J. Organomet. Chem.* **2010**, *695*, 201−205.

(36) (a) Ashby, E. C.; Coleman, D. Evidence for Single Electron Transfer in the Reactions of Lithium Dimethylcuprate with Alkyl Halides. *J. Org. Chem.* **1987**, *52*, 4554−4565. (b) Hill, E. A.; Hsieh, K.; Condroski, K.; Sonnentag, H.; Skalitzky, D.; Gagas, D. Rearrangement and Cleavage of the Grignard Reagent from 5-(Chloromethyl)norbornene. *J. Org. Chem.* **1989**, *54*, 5286−5292. (c) Das, A.; Hua, Y.; Yousufuddin, M.; Cundari, T. R.; Jeon, J.; Dias, H. V. R. Gold-Mediated Isomerization of Cyclooctyne to Ring Fused Olefinic Bicycles. *Eur. J. Inorg. Chem.* **2016**, *2016*, 995−1001.

(37) Becker, K. B. The Synthesis of Cycloalkenes by the Intramolecular Wittig Reaction. *Helv. Chim. Acta* **1977**, *60*, 68−80.

(38) Negishi, E.; Sawada, H.; Tour, J. M.; Wei, Y. Novel Bicyclization Methodology via Cyclialkylation of ω-Halo-1-metallo-1-alkynes Containing Aluminum and Zinc. *J. Org. Chem.* **1988**, *53*, 913−915.

(39) Perdriau, S.; Chang, M.-C.; Otten, E.; Heeres, H. J.; de Vries, J. G. Alkene Isomerisation Catalysed by a Ruthenium PNN Pincer Complex. *Chem. Eur. J.* **2014**, *20*, 15434−15442.

(40) Wu, X.; Xiao, G.; Ding, Y.; Zhan, Y.; Zhao, Y.; Chen, R.; Loh, T.-P. Palladium-Catalyzed Intermolecular Polarity-Mismatched Addition of Unactivated Alkyl Radicals to Unactivated Alkenes. *ACS Catal.* **2020**, *10*, 14107−14116.

(41) (a) Guthrie, J. P.; Guo, J. Intramolecular Aldol Condensations: Rate and Equilibrium Constants. *J. Am. Chem. Soc.* **1996**, *118*, 11472−11487. (b) Brinker, U. H.; Lin, G.; Xu, L.; Smith, W. B.; Mieusset, J.-L. Dihalocarbene Insertion Reactions into C−H Bonds of Compounds Containing Small Rings: Mechanisms and Regio- and Stereoselectivities. *J. Org. Chem.* **2007**, *72*, 8434−8451.

(42) Nugent, W. A.; Feldman, J.; Calabrese, J. C. Practical Catalyst for Cyclic Metathesis. Synthesis of Functional and/or Enantiopure Cycloalkenes. *J. Am. Chem. Soc.* **1995**, *117*, 8992−8998.

(43) Okada, T.; Takeuchi, D.; Shishido, A.; Ikeda, T.; Osakada, K. Isomerization Polymerization of 4-Alkylcyclopentenes Catalyzed by Pd Complexes: Hydrocarbon Polymers with Isotactic-Type Stereochemistry and Liquid-Crystalline Properties. *J. Am. Chem. Soc.* **2009**, *131*, 10852−10853.

https://doi.org/10.1021/acs.organomet.1c00694
Organometallics 2022, 41, 345−353